Linking source and sink: The timing of deposition of Paleogene syntectonic strata in Central Asia

Feng Cheng[1,2,*], Andrew V. Zuza[3], Marc Jolivet[4], Andreas Mulch[2,5], Niels Meijer[4], Zhaojie Guo[1]

[1] *Key Laboratory of Orogenic Belts and Crustal Evolution, Ministry of Education, School of Earth and Space Sciences, Peking University, Beijing, China*

[2] *Senckenberg Biodiversity and Climate Research Centre, Frankfurt am Main, Germany*

[3] *Nevada Bureau of Mines and Geology, University of Nevada, Reno, NV 89557, USA*

[4] *Géosciences Rennes–UMR CNRS 6118, Univ Rennes, 35000 Rennes, France*

[5] *Institute of Geosciences, Goethe University Frankfurt, Frankfurt am Main, Germany*

* Correspondence: cfcf.chengfeng@gmail.com

Supplementary Materials

This file includes:

Test S1. Geological background of the Zagros fold-and-thrust belt and Ruby Mountains metamorphic core complex

The NW trending Zagros fold-and-thrust belt (hereafter Zagros), built on the original passive continental margin of the Arabian plate, forms as a result of the closure of Neo-Tethys and convergence between the Arabian and Eurasian plates (Koshnaw et al., 2020a; Koshnaw et al., 2020b) (Fig. S1). In the foreland basin of the Zagros, the deposition ages of Neogene strata Injan (~12.4-7.75 Ma), Mukdadiya (~7.75-5 Ma), and Bai-Hasan (<5 Ma) formations have been well-dated based on the magnetostratigraphy study together with independent ages derived from fossils and the youngest detrital zircon U-Pb age constraints (Koshnaw et al., 2020a)(Fig. 2E). In respond to the crustal shortening, the pulsed southwestward propagation of the thrust belts in the Zagros (e.g., Kirkuk fault) are constrained by the field investigation, petroleum exploration and LTT (Koshnaw et al., 2017)(Fig. 2E-2G). Thermochronological and associated thermal history modeling studies on basement rocks on the hanging wall of Kirkuk Fault reveal a rapid reverse-faulting exhumation at 8-7 Ma (Koshnaw et al., 2020b)(Fig. 2G-2H).

Located in the northeastern Nevada, western America, the NE trending Ruby Mountains metamorphic core complex (Ruby Mts.) has played a significant role in Basin and Range extension (Fig. S2). The current morphology of these ranges is mainly established due to the middle Miocene to present extension which associated with deposition of Miocene-present basins (Colgan et al., 2010). In addition to the age constraints on underlying Oligocene basal tuffaceous sediments, the depositional age of the Humboldt Fm. (~16 Ma to <8 Ma) is well-constrained based on the $^{40}Ar/^{39}Ar$ dating and detrital zircon geochronology (Lund Snee et al., 2016)(Fig. 2H-2J). Apatite fission track (AFT) and AHe ages from the footwall of the Ruby detachment record rapid cooling from >120°C to <40°C during a relatively narrow window in the middle Miocene, with best fit t-T paths clustering around 17–15 Ma (Colgan et al., 2010). Thus, the Ruby Mts experience a rapid extensional exhumation at the middle Miocene. Note that the low-temperature thermochronology data from the Ruby mountains are interpreted from thermal models while the data from the Zagros are weighted mean dates (Fig. 2).

Test S2. Details of the statistical analyses of the Paleogene tectonism in the northern Tibetan plateau

To investigate the Paleogene tectonism in the northern Tibetan plateau, we combined the newly constrained syntectonic sedimentary records in and around the Qaidam basin with the published Low-temperature thermochronology (LTT) datasets reflecting Paleogene mountain-building in Northern Tibet. By applying our new approach to debated age model of the Cenozoic strata in the Qaidam basin, we have defined the timing of the Paleogene syntectonic sedimentary records in and around the Qaidam basin, ranging from 59 Ma to 30 Ma. Additionally. We compiled rapid cooling ages of the apatite fission track and (U-Th)/He results from the published thermochronology datasets, resulting in a total of 111 ages that represent the timing of Paleogene tectonic activity in Northern Tibet (Table S1).

We recognize that LTT records provide constrains only on the range exhumation, and that climate effects can also contribute to rapid exhumation of basement rocks in addition to the tectonic activity (Nie et al., 2018; Ye et al., 2022). However, we do not observe a correlation between global climate events (as shown in Fig. 4) and the LTT compilation. Furthermore, it has been suggested that erosion has driven exhumation in regions with high precipitation such as the Himalayas and southern Pamir, but North Tibet and Central Asia are considered too dry (Jepson et al., 2021). Hence, most studies attribute these Paleogene LTT records to the rock uplift of the basements in Northern Tibet, rather than climate effects alone (Cao et al., 2015; Cao et al., 2013; Clark et al., 2010; He et al., 2017; He et al., 2018; He et al., 2021; He et al., 2022; Jolivet et al., 2001; Li et al., 2023; Li et al., 2021; Li et al., 2019; Staisch et al., 2020; Wang et al., 2017; Zhuang et al., 2018). We thus consider these LTT data to be indicative of the mountain-building activity in the Northern Tibet. For instance, thermochronological and associated thermal history modeling studies on basement rocks of Altyn Tagh Range (See Section QB1 in Fig. 3A) reveal rapid exhumation episodes during two periods: ca. 50-30 Ma and ca. 30-10 Ma (Jolivet et al., 2001; Zhang et al., 2012). Based on the (U-Th)/He ages derived from apatite samples collected along the elevation transects across the Eastern Kunlun Shan, Clark et al. (2010) and Li et al. (2021) reveal a rapid cooling event of the basement rock of Eastern Kunlun Shan at ca. 35-25 Ma (See Section QB2 in Fig. 3B). This accelerated cooling, according to both Clark et al. (2010) and Li et al. (2021) is attributed primarily to rock uplift rather than shifts in climate. The exhumation rate experienced a remarkable acceleration at ca. 35-25 Ma, increasing from ca. 0.03 mm/yr to 0.40-0.50 mm/yr ca. 35-25 Ma. A histogram diagram of the timing of Paleogene tectonic activity in the northern Tibetan plateau is then generated using Origin 10.5 software (Fig. 4D), with the bin width of 1.5 million years. Note that the low-temperature thermochronology data from the Eastern Kunlun Shan, Altyn Tagh Range are interpreted from thermal models (Fig. 2).

Test S3. Growth of Pamir vs. Proto-Paratethys Sea retreat

Geologists have been intrigued for years by how the Proto-Paratethys Sea retreated from Central Asia, as this offers valuable insights into biodiversity and climate change(Blayney et al., 2019; Bosboom et al., 2017; Bougeois et al., 2018; Dupont-Nivet et al., 2007; Kaya et al., 2019; Meijer et al., 2019). While some experts attribute the fluctuations of the Proto-Paratethys Sea to tectonic and eustatic factors, as evidenced by several studies (Bosboom et al., 2017; Burtman and Molnar, 1993; Dupont-Nivet et al., 2007) (Fig. 4A-4D), the Tarim Sea level fluctuations in the Paleogene (Fig. 4C) do not align with eustatic change (Fig. 4A) or with global and regional climate change (Fig. S3). Therefore, it is likely that tectonic factor played dominant role in the evolution and demise of the Proto-Paratethys Sea during the Paleogene.

Previous studies have suggested that the uplift and northward indentation of the Pamir salient, situated between the Neotethys Ocean and the Tarim Sea during the Paleogene, ultimately led to the demise of the Proto-Paratethys Sea (Blayney et al., 2016; Kaya et al., 2019; Sun et al., 2017). Although some records of accelerated exhumation and crustal thickening during the Paleocene to Eocene in the Pamir and Western Kunlun Shan have been reported (Amidon and Hynek, 2010; Chapman et al., 2018; Ducea et al., 2003; Hacker et al., 2005; Li et al., 2019), Oligocene-Miocene and Pliocene tectonism evidenced by the LTT are predominant in this region (Cao et al., 2015; Chen et al., 2021; Jepson et al., 2021). For instance, thermochronological and associated thermal history modeling studies on basement rocks of Western Kunlun Shan along section TB1(Fig. 3C) reveal a prominent latest Oligocene-Miocene (24-12 Ma and 12-6 Ma) cooling of the exhumation (Li et al., 2019). Meanwhile, thermochronological and associated thermal history modeling results on basement rocks of Western Kunlun Shan along section TB2 (Fig. 3D) shows a widespread Miocene to Pliocene (ca. 15-5 Ma) cooling of the exhumation (Cao et al., 2015). Given the relatively limited LTT records that reproduce the Paleogene rock uplift history of the Pamir region (Jepson et al., 2021), it remains speculative how the Paleogene tectonism in the Pamir region controlled the evolution of the Proto-Paratethys Sea.

On the other hand, recent reports of Paleogene marine records in the Qaidam basin indicate that the Proto-Paratethys Sea might have extended further eastward into Northern Tibet (Ma et al., 2022)(Fig. 1B). Therefore, the Paleogene intracontinental deformation along North Tibet could play a crucial role in the Proto-Paratethys Sea's retreat (Kaya et al., 2019). Furthermore, several records of Paleogene tectonism (e.g., LTT) in Northern Tibet have been reported (Table S1). By combining the newly constrained syntectonic sedimentary records in and around the Qaidam basin with the published LTT datasets reflecting Paleogene mountain-building in Northern Tibet, we can qualitatively investigate the link between the Paleogene tectonism in Northern Tibet and the evolution of the Proto-Paratethys Sea (Fig. S3). We propose that renewed acceleration of deformation in Northern Tibet and associated surface elevation change promoted the intermittent retreat of the Proto-Paratethys Sea, while intervening deceleration of tectonic deformation facilitated Proto-Paratethys Sea incursions. The relatively subdued relief in Northern Tibet shortly after the India-Asia collision may have promoted the 1st Proto-Paratethys Sea incursion. The renewed acceleration of deformation (and proposed small-scale surface uplift) from 56 Ma to 48 Ma, at 41-39 Ma and at ca. 36 Ma compensated for the general rise of eustatic sea level, resulting in the 1st, 2nd and 3rd regression, respectively. On the other hand, when the eustatic sea level remained relatively constant from 48 Ma to 41 Ma and from 39 Ma to 36 Ma, lower magnitudes of deformation may have contributed to facilitating the 2nd and 3rd incursion (Fig. 4D). We note that the 3rd regression of the Proto-Paratethys Sea predates the extensive Miocene deformation in the northern Tibetan plateau and Pamir, but roughly coincides with the late Eocene to early Oligocene deformation in the northern Tibet (Fig. 4D). We infer that the late Eocene to early Oligocene tectonics deformation (e.g., uplift and basin infilling) in the Pamir and northern Tibetan plateau and the global sea level fall during the

Eocene-Oligocene Transition contributed to the demise of the Proto-Paratethys Sea from Central Asia (Kaya et al., 2019).

Test S4. Cenozoic offset along the Altyn Tagh fault

The Altyn Tagh fault is a lithospheric sinistral strike-slip fault that extends for over 1600 km from the Western Kunlun Shan, through the Altyn Tagh Range, and to the northwestern end of the Qilian Shan, separating the Tibetan plateau from the Tarim basin (Burchfiel et al., 1989; Cheng et al., 2019a; Cheng et al., 2015b; Yin et al., 2002)(Fig. 1). This fault has accommodated hundreds of kilometers of the post-collisional convergence between India and Asia through left-lateral offset(Cheng et al., 2017; Cowgill et al., 2003; Delville et al., 2001; Meyer et al., 1996; Yin and Harrison, 2000). The cumulative left-lateral displacement estimates generally range from ca. 300 to ca. 500 km(Chen et al., 2002; Cheng et al., 2015a; Cheng et al., 2015b; Cheng et al., 2016; Cowgill et al., 2003; Meng et al., 2001; Ritts and Biffi, 2000; Wu et al., 2012; Yue et al., 2005; Zhuang et al., 2018), while the proposed Cenozoic initiation of sinistral faulting along the Altyn Tagh fault varies from Paleocene-Eocene to Miocene (Cheng et al., 2015a; Cheng et al., 2016; Cheng et al., 2019b; Jolivet et al., 2001; Wu et al., 2012; Yin et al., 2008; Yin et al., 2002; Yue et al., 2001).

The large-scale displacement along the Altyn Tagh fault during the Paleocene to Oligocene suggests that Northern Tibet was situated closer to the SW Tarim basin. However, the LTT data shows that exhumation within the Altyn Tagh Range was minor during the Paleocene-Eocene(Jepson et al., 2021; Jolivet et al., 2001; Wang et al., 2015; Yin et al., 2002). On the other hand, the tectonic activity within the Altyn Tagh Range was intensified mountain-building during the Oligocene-Miocene(Jolivet et al., 1999; Sobel et al., 2001; Wang et al., 2006; Ye et al., 2022; Yu et al., 2019). We thus suggest that the Proto-Paratethys Sea would overcome the minor deformation and minor relief in the Altyn Tagh Range, extending further eastward into the Northern Tibet during the Paleogene(Ma et al., 2022; Meng and Fang, 2008).

Figure S1. Geological map of Zagros fold-thrust belt. (A) Index map of the Zagros region, showing the location of the studied area. (B) Geological map of Zagros and the surrounding regions, modified from Koshnaw et al. (2017). Note the locations of seismic profile are from Koshnaw et al. (2017) and Koshnaw et al. (2020b) the LTT results are from Koshnaw et al. (2020b).

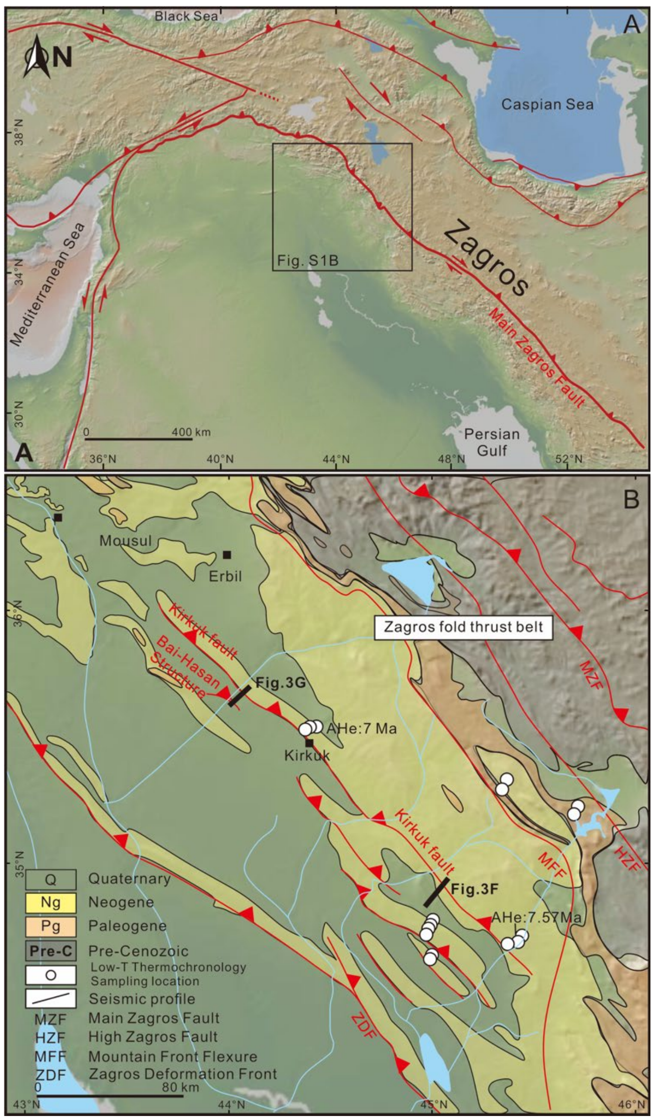

Figure S2. Geological map of Ruby Mountains metamorphic core complex. (A) Index map of the Great Basin region, showing the location of the studied area. (B) Geological map of Ruby Mountains, NE Nevada, and the surrounding regions, modified from Lund Snee et al. (2016). Note the locations of seismic profile are from Satarugsa and Johnson (2000) and the apatite fission track and (U-Th)/He results are from Colgan et al. (2010).

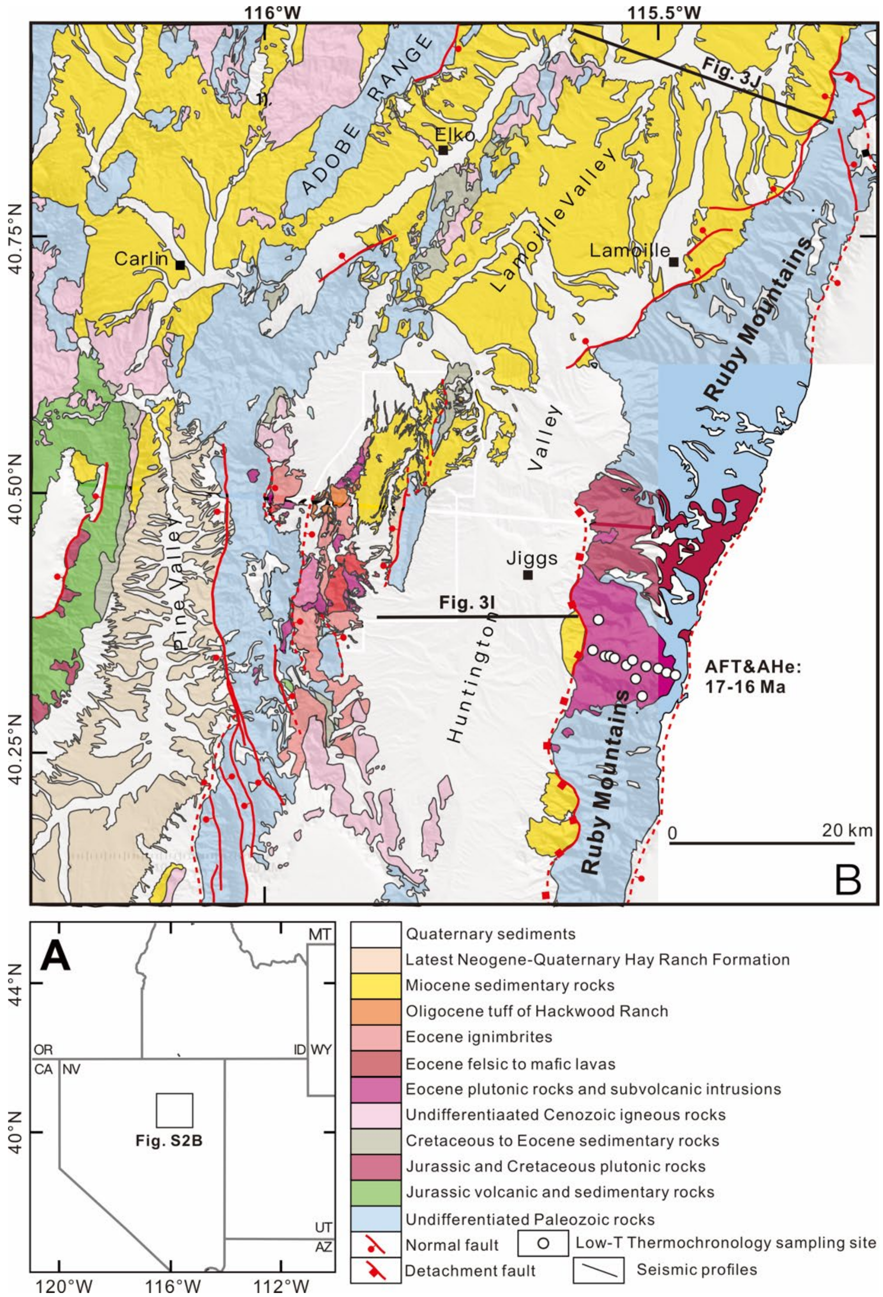

Figure S3. Proto-Paratethys Sea fluctuation vs. regional/global climate change and tectonism. (A) Global benthic $\delta^{18}O$ stack (Westerhold et al., 2020). (B) Global sea level (Miller et al., 2020). (C) (Smectite+Illite/Smectite)/Illite ratios in Xining and Qaidam basins, indicating a long-term decrease of silicate weathering intensity (Fang et al., 2019; Ye et al., 2016). (D) Tectonic data are compiled from Kaya et al. (2019) and references therein. (E) Tarim Sea level fluctuation (Kaya et al., 2019). (F) Histogram of the timing of tectonic events in the northern Tibet. The timing of tectonic activities is from He et al. (2018) and Table S1.

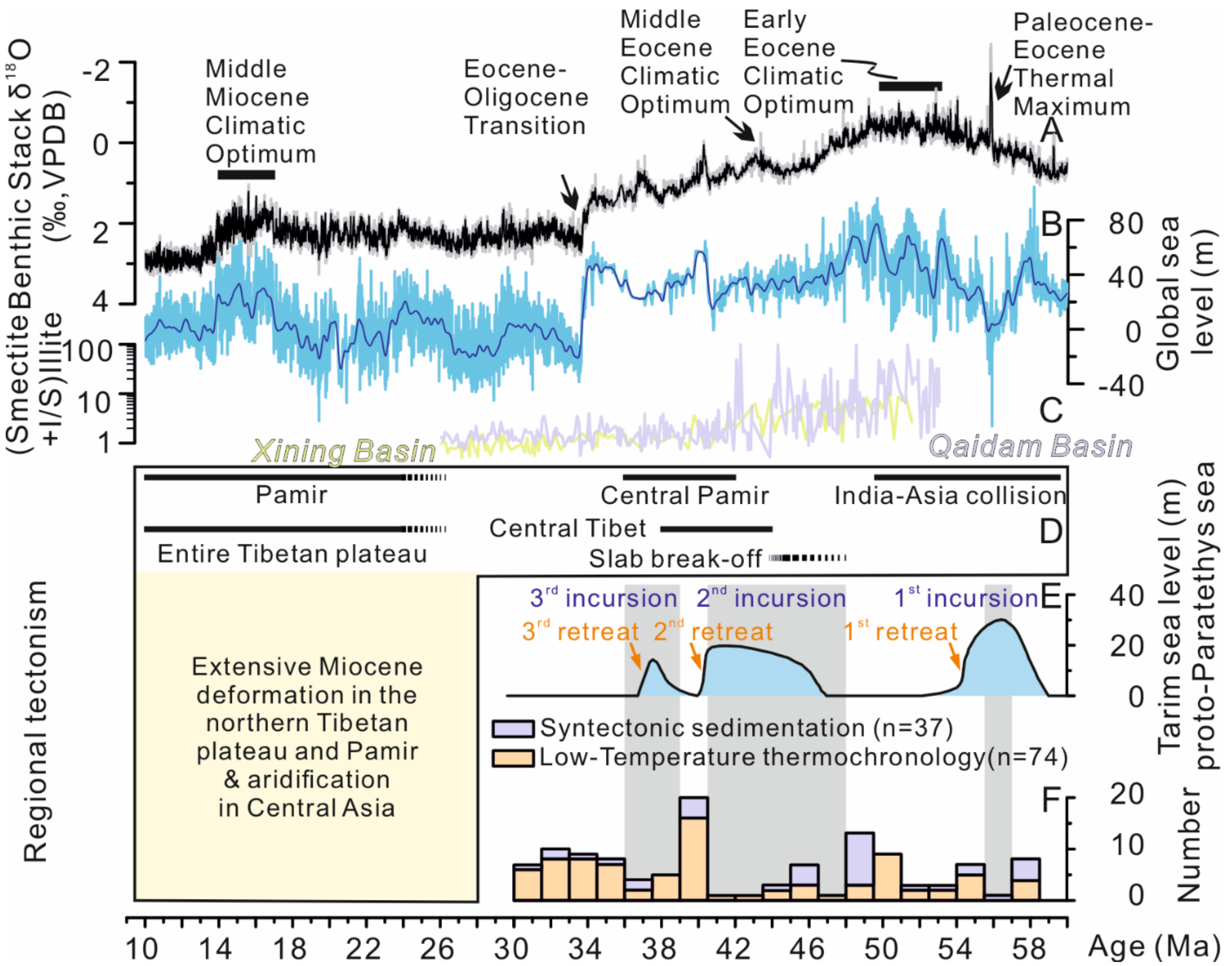

Figure S4. Conceptual model of Proto-Paratethys Sea evolution. (A) Paleogene period, (B) Present-day. Given the 300-500 km left-slip offset along the Altyn Tagh fault since the

Eocene(Cheng et al., 2016), the Northern Tibet was situated closer to the SW Tarim basin and the Proto-Paratethys Sea might transgress across the Altyn Tagh Range, extending further eastward into Northern Tibet during the Paleogene.

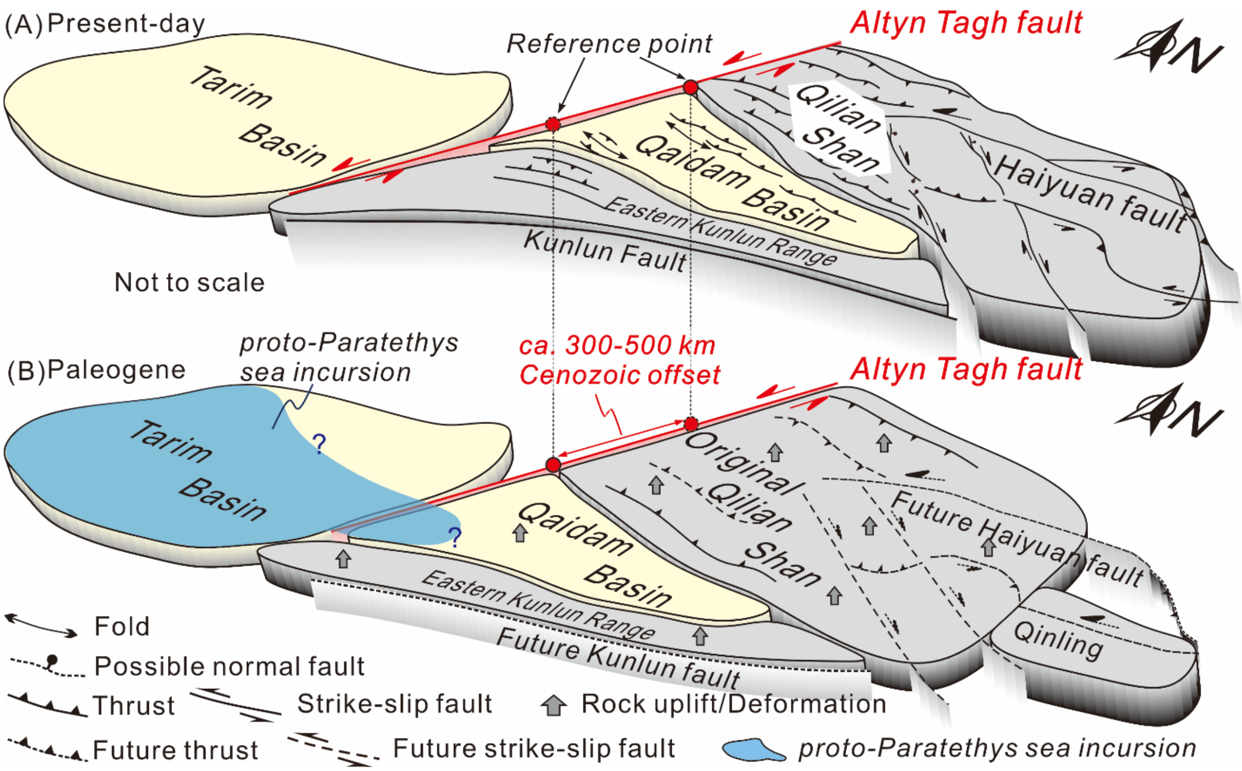

Table S1. Compilation of published Paleogene tectonic events in the northern Tibetan plateau.

REFERENCES CITED

Amidon, W. H., and Hynek, S. A., 2010, Exhumational history of the north central Pamir: Tectonics, v. 29, no. 5.

Blayney, T., Dupont-Nivet, G., Najman, Y., Proust, J.-N., Meijer, N., Roperch, P., Sobel, E. R., Millar, I., and Guo, Z., 2019, Tectonic Evolution of the Pamir Recorded in the Western Tarim Basin (China): Sedimentologic and Magnetostratigraphic Analyses of the Aertashi Section: Tectonics, v. 38, no. 2, p. 492-515.

Blayney, T., Najman, Y., Dupont-Nivet, G., Carter, A., Millar, I., Garzanti, E., Sobel, E. R., Rittner, M., Andò, S., Guo, Z., and Vezzoli, G., 2016, Indentation of the Pamirs with respect to the northern margin of Tibet: Constraints from the Tarim basin sedimentary record: Tectonics, v. 35, no. 10, p. 2345-2369.

Bosboom, R., Mandic, O., Dupont-Nivet, G., Proust, J.-N., Ormukov, C., and Aminov, J., 2017, Late Eocene palaeogeography of the proto-Paratethys Sea in Central Asia (NW China, southern Kyrgyzstan and SW Tajikistan): Geological Society, London, Special Publications, v. 427, no. 1, p. 565-588.

Bougeois, L., Dupont-Nivet, G., de Rafélis, M., Tindall, J. C., Proust, J.-N., Reichart, G.-J., de Nooijer, L. J., Guo, Z., and Ormukov, C., 2018, Asian monsoons and aridification response to Paleogene sea retreat and Neogene westerly shielding indicated by seasonality in Paratethys oysters: Earth and Planetary Science Letters, v. 485, p. 99-110.

Burchfiel, B. C., Quidong, D., Molnar, P., Royden, L., Yipeng, W., Peizhen, Z., and Weiqi, Z., 1989, Intracrustal detachment within zones of continental deformation: Geology, v. 17, no. 8, p. 748-752.

Burtman, V. S., and Molnar, P., 1993, Geological and Geophysical Evidence for Deep Subduction of Continental Crust Beneath the Pamir, *in* Burtman, V. S., and Molnar, P., eds., Geological and Geophysical Evidence for Deep Subduction of Continental Crust Beneath the Pamir, Volume 281, Geological Society of America, p. 0.

Cao, K., Wang, G.-C., Bernet, M., van der Beek, P., and Zhang, K.-X., 2015, Exhumation history of the West Kunlun Mountains, northwestern Tibet: Evidence for a long-lived, rejuvenated orogen: Earth and Planetary Science Letters, v. 432, p. 391-403.

Cao, K., Wang, G.-C., van der Beek, P., Bernet, M., and Zhang, K.-X., 2013, Cenozoic thermo-tectonic evolution of the northeastern Pamir revealed by zircon and apatite fission-track thermochronology: Tectonophysics, v. 589, p. 17-32.

Chapman, J. B., Scoggin, S. H., Kapp, P., Carrapa, B., Ducea, M. N., Worthington, J., Oimahmadov, I., and Gadoev, M., 2018, Mesozoic to Cenozoic magmatic history of the Pamir: Earth and Planetary Science Letters, v. 482, p. 181-192.

Chen, H., Lin, X., Cheng, X., Gong, J., Bian, S., Wu, L., Jia, C., Yang, S., Guo, Z., and Jia, D., 2021, Two-phase intracontinental deformation mode in the context of India–Eurasia collision: insights from a structural analysis of the West Kunlun–Southern Junggar transect along the NW margin of the Tibetan Plateau: Journal of the Geological Society, v. 179, no. 2, p. jgs2021-2029.

Chen, Y., Gilder, S., Halim, N., Cogné, J. P., and Courtillot, V., 2002, New paleomagnetic constraints on central Asian kinematics: Displacement along the Altyn Tagh fault and rotation of the Qaidam Basin: Tectonics, v. 21, no. 5, p. 1042.

Cheng, F., Garzione, C., Jolivet, M., Wang, W., Dong, J., Richter, F., and Guo, Z., 2019a, Provenance analysis of the Yumen Basin and northern Qilian Shan: Implications for the pre-collisional paleogeography in the NE Tibetan plateau and eastern termination of Altyn Tagh fault: Gondwana Research, v. 65, p. 156-171.

Cheng, F., Guo, Z., Jenkins, H. S., Fu, S., and Cheng, X., 2015a, Initial rupture and displacement on the Altyn Tagh fault, northern Tibetan Plateau: Constraints based on residual Mesozoic to Cenozoic strata in the western Qaidam Basin: Geosphere, v. 11, no. 3, p. 921-942.

Cheng, F., Jolivet, M., Dupont-Nivet, G., Wang, L., Yu, X., and Guo, Z., 2015b, Lateral extrusion along the Altyn Tagh Fault, Qilian Shan (NE Tibet): insight from a 3D crustal budget: Terra Nova, v. 27, no. 6, p. 416-425.

Cheng, F., Jolivet, M., Fu, S., Zhang, C., Zhang, Q., and Guo, Z., 2016, Large-scale displacement along the Altyn Tagh Fault (North Tibet) since its Eocene initiation: Insight from detrital zircon U–Pb geochronology and subsurface data: Tectonophysics, v. 677–678, p. 261-279.

Cheng, F., Jolivet, M., Guo, Z., Lu, H., Zhang, B., Li, X., Zhang, D., Zhang, C., Zhang, H., Wang, L., Wang, Z., and Zhang, Q., 2019b, Jurassic–Early Cenozoic Tectonic Inversion in the Qilian Shan and Qaidam Basin, North Tibet: New Insight From Seismic Reflection, Isopach Mapping, and Drill Core Data: Journal of Geophysical Research: Solid Earth, v. 124, no. 11, p. 12077-12098.

Cheng, F., Jolivet, M., Hallot, E., Zhang, D., Zhang, C., and Guo, Z., 2017, Tectono-magmatic rejuvenation of the Qaidam craton, northern Tibet: Gondwana Research, v. 49, p. 248-263.

Clark, M., Farley, K., Zheng, D., Wang, Z., and Duvall, A., 2010, Early Cenozoic faulting of the northern Tibetan Plateau margin from apatite (U–Th)/He ages: Earth and Planetary Science Letters, v. 296, no. 1, p. 78-88.

Colgan, J. P., Howard, K. A., Fleck, R. J., and Wooden, J. L., 2010, Rapid middle Miocene extension and unroofing of the southern Ruby Mountains, Nevada: Tectonics, v. 29, no. 6.

Cowgill, E., Yin, A., Harrison, T. M., and Xiao-Feng, W., 2003, Reconstruction of the Altyn Tagh fault based on U-Pb geochronology: Role of back thrusts, mantle sutures, and heterogeneous crustal strength in forming the Tibetan Plateau: Journal of Geophysical Research, v. 108, no. B7, p. 2346.

Delville, N., Arnaud, N., Montel, J.-M., Roger, F., Brunel, M., Tapponnier, P., and Sobel, E., 2001, Paleozoic to Cenozoic deformation along the Altyn Tagh fault in the Altun Shan massif area, eastern Qilian Shan, northeastern Tibet, China: Geological Society of America Memoirs, v. 194, p. 269-292.

Ducea, M. N., Lutkov, V., Minaev, V. T., Hacker, B., Ratschbacher, L., Luffi, P., Schwab, M., Gehrels, G. E., McWilliams, M., Vervoort, J., and Metcalf, J., 2003, Building the Pamirs: The view from the underside: Geology, v. 31, no. 10, p. 849-852.

Dupont-Nivet, G., Krijgsman, W., Langereis, C. G., Abels, H. A., Dai, S., and Fang, X., 2007, Tibetan plateau aridification linked to global cooling at the Eocene–Oligocene transition: Nature, v. 445, no. 7128, p. 635-638.

Fang, X., Galy, A., Yang, Y., Zhang, W., Ye, C., and Song, C., 2019, Paleogene global cooling–induced temperature feedback on chemical weathering, as recorded in the northern Tibetan Plateau: Geology, v. 47, no. 10, p. 992-996.

Hacker, B., Luffi, P., Lutkov, V., Minaev, V., Ratschbacher, L., Plank, T., Ducea, M., PatiÑO-Douce, A., McWilliams, M., and Metcalf, J. I. M., 2005, Near-Ultrahigh Pressure Processing of Continental Crust: Miocene Crustal Xenoliths from the Pamir: Journal of Petrology, v. 46, no. 8, p. 1661-1687.

He, P., Song, C., Wang, Y., Chen, L., Chang, P., Wang, Q., and Ren, B., 2017, Cenozoic exhumation in the Qilian Shan, northeastern Tibetan Plateau: Evidence from detrital fission track thermochronology in the Jiuquan Basin: Journal of Geophysical Research: Solid Earth, v. 122, no. 8, p. 6910-6927.

He, P., Song, C., Wang, Y., Meng, Q., Chen, L., Yao, L., Huang, R., Feng, W., and Chen, S., 2018, Cenozoic deformation history of the Qilian Shan (northeastern Tibetan Plateau) constrained by detrital apatite fission-track thermochronology in the northeastern Qaidam Basin: Tectonophysics, v. 749, p. 1-11.

He, P., Song, C., Wang, Y., Wang, D., Chen, L., Meng, Q., and Fang, X., 2021, Early Cenozoic activated deformation in the Qilian Shan, northeastern Tibetan Plateau: Insights from detrital apatite fission-track analysis: Basin Research, v. 33, no. 3, p. 1731-1748.

He, P., Song, C., Wang, Y., Zhao, Y., Tan, Y., Meng, Q., Zhang, Y., Chen, Y., and Zhang, J., 2022, Cenozoic two-phase topographic growth of the northeastern Tibetan Plateau derived from two thermochronologic transects across the southern Qilian Shan thrust belt: Tectonophysics, v. 837, p. 229432.

Jepson, G., Carrapa, B., Gillespie, J., Feng, R., DeCelles, P. G., Kapp, P., Tabor, C. R., and Zhu, J., 2021, Climate as the Great Equalizer of Continental-Scale Erosion: Geophysical Research Letters, v. 48, no. 20, p. e2021GL095008.

Jolivet, M., Brunel, M., Seward, D., Xu, Z., Yang, J., Roger, F., Tapponnier, P., Malavieille, J., Arnaud, N., and Wu, C., 2001, Mesozoic and Cenozoic tectonics of the northern edge of the Tibetan plateau: fission-track constraints: Tectonophysics, v. 343, no. 1-2, p. 111-134.

Jolivet, M., Roger, F., Arnaud, N., Brunel, M., Tapponnier, P., and Seward, D., 1999, Histoire de l'exhumation de l'Altun Shan: indications sur l'âge de la subduction du bloc du Tarim sous le système de l'Altyn Tagh (Nord Tibet): Comptes Rendus de l'Académie des Sciences-Series IIA-Earth and Planetary Science, v. 329, no. 10, p. 749-755.

Kaya, M. Y., Dupont-Nivet, G., Proust, J.-N., Roperch, P., Bougeois, L., Meijer, N., Frieling, J., Fioroni, C., Özkan Altıner, S., Vardar, E., Barbolini, N., Stoica, M., Aminov, J., Mamtimin, M., and Zhaojie, G., 2019, Paleogene evolution and demise of the proto-Paratethys Sea in Central Asia (Tarim and Tajik basins): Role of intensified tectonic activity at ca. 41 Ma: Basin Research, v. 31, no. 3, p. 461-486.

Koshnaw, R. I., Horton, B. K., Stockli, D. F., Barber, D. E., and Tamar-Agha, M. Y., 2020a, Sediment routing in the Zagros foreland basin: Drainage reorganization and a shift from axial to transverse sediment dispersal in the Kurdistan region of Iraq: Basin Research, v. 32, no. 4, p. 688-715.

Koshnaw, R. I., Horton, B. K., Stockli, D. F., Barber, D. E., Tamar-Agha, M. Y., and Kendall, J. J., 2017, Neogene shortening and exhumation of the Zagros fold-thrust belt and foreland basin in the Kurdistan region of northern Iraq: Tectonophysics, v. 694, p. 332-355.

Koshnaw, R. I., Stockli, D. F., Horton, B. K., Teixell, A., Barber, D. E., and Kendall, J. J., 2020b, Late Miocene Deformation Kinematics Along the NW Zagros Fold-Thrust Belt, Kurdistan Region of Iraq: Constraints From Apatite (U-Th)/He Thermochronometry and Balanced Cross Sections: Tectonics, v. 39, no. 12, p. e2019TC005865.

Li, C., Zheng, D., Yu, J., Zhou, R., Wang, Y., Pang, J., Wang, Y., Hao, Y., and Xu, Y.-G., 2023, Late Oligocene mountain building of the East Kunlun Shan in northeastern Tibet: Impact on the Cenozoic climate evolution in East Asia: Global and Planetary Change, v. 224, p. 104114.

Li, C., Zheng, D., Zhou, R., Yu, J., Wang, Y., Pang, J., Wang, Y., Hao, Y., and Li, Y., 2021, Late Oligocene Tectonic Uplift of the East Kunlun Shan: Expansion of the Northeastern Tibetan Plateau: Geophysical Research Letters, v. 48, no. 3, p. e2020GL091281.

Li, G., Sandiford, M., Fang, A., Kohn, B., Sandiford, D., Fu, B., Zhang, T., Cao, Y., and Chen, F., 2019, Multi-stage exhumation history of the West Kunlun orogen and the amalgamation of the Tibetan Plateau: Earth and Planetary Science Letters, v. 528, p. 115833.

Lund Snee, J. E., Miller, E. L., Grove, M., Hourigan, J. K., and Konstantinou, A., 2016, Cenozoic paleogeographic evolution of the Elko Basin and surrounding region, northeast Nevada: Geosphere, v. 12, no. 2, p. 464-500.

Ma, J., Wu, C., Uveges, B. T., Ding, W., Summons, R. E., and Cui, X., 2022, Biomarkers reveal Eocene marine incursions into the Qaidam Basin, north Tibetan Plateau: Organic Geochemistry, v. 166, p. 104380.

Meijer, N., Dupont-Nivet, G., Abels, H. A., Kaya, M. Y., Licht, A., Xiao, M., Zhang, Y., Roperch, P., Poujol, M., Lai, Z., and Guo, Z., 2019, Central Asian moisture modulated by proto-Paratethys Sea incursions since the early Eocene: Earth and Planetary Science Letters, v. 510, p. 73-84.

Meng, Q. R., and Fang, X., 2008, Cenozoic tectonic development of the Qaidam Basin in the northeastern Tibetan Plateau: Geological Society of America Special Paper, v. 444, p. 1-24.

Meng, Q. R., Hu, J. M., and Yang, F. Z., 2001, Timing and magnitude of displacement on the Altyn Tagh fault: constraints from stratigraphic correlation of adjoining Tarim and Qaidam basins, NW China: Terra Nova, v. 13, no. 2, p. 86-91.

Meyer, B., Tapponnier, P., Gaudemer, Y., Peltzer, G., Shunmin, G., and Zhitai, C., 1996, Rate of left-lateral movement along the easternmost segment of the Altyn Tagh fault, east of 96° E (China): Geophysical Journal International, v. 124, no. 1, p. 29-44.

Miller, K. G., Browning, J. V., Schmelz, W. J., Kopp, R. E., Mountain, G. S., and Wright, J. D., 2020, Cenozoic sea-level and cryospheric evolution from deep-sea geochemical and continental margin records: Science Advances, v. 6, no. 20, p. eaaz1346.

Nie, J., Ruetenik, G., Gallagher, K., Hoke, G., Garzione, C. N., Wang, W., Stockli, D., Hu, X., Wang, Z., and Wang, Y., 2018, Rapid incision of the Mekong River in the middle Miocene linked to monsoonal precipitation: Nature Geoscience, v. 11, no. 12, p. 944.

Ritts, B. D., and Biffi, U., 2000, Magnitude of post-Middle Jurassic (Bajocian) displacement on the central Altyn Tagh fault system, northwest China: Geological Society of America Bulletin, v. 112, no. 1, p. 61-74.

Satarugsa, P., and Johnson, R. A., 2000, Cenozoic tectonic evolution of the Ruby Mountains metamorphic core complex and adjacent valleys, northeastern Nevada: Rocky Mountain Geology, v. 35, no. 2, p. 205-230.

Sobel, E. R., Arnaud, N., Jolivet, M., Ritts, B. D., and Brunel, M., 2001, Jurassic to Cenozoic exhumation history of the Altyn Tagh range, northwest China, constrained by 40Ar/39Ar and apatite fission track thermochronology: Geological Society of America Memoirs, v. 194, p. 247-267.

Staisch, L. M., Niemi, N. A., Clark, M. K., and Chang, H., 2020, The Cenozoic Evolution of Crustal Shortening and Left-Lateral Shear in the Central East Kunlun Shan: Implications for the Uplift History of the Tibetan Plateau: Tectonics, v. 39, no. 9, p. e2020TC006065.

Sun, J., Liu, W., Liu, Z., Deng, T., Windley, B. F., and Fu, B., 2017, Extreme aridification since the beginning of the Pliocene in the Tarim Basin, western China: Palaeogeography, Palaeoclimatology, Palaeoecology, v. 485, no. Supplement C, p. 189-200.

Wang, E., Xu, F.-Y., Zhou, J.-X., Wan, J., and Burchfiel, B. C., 2006, Eastward migration of the Qaidam basin and its implications for Cenozoic evolution of the Altyn Tagh fault and associated river systems: Geological Society of America Bulletin, v. 118, no. 3-4, p. 349-365.

Wang, F., Shi, W., Zhang, W., Wu, L., Yang, L., Wang, Y., and Zhu, R., 2017, Differential growth of the northern Tibetan margin: evidence for oblique stepwise rise of the Tibetan Plateau: Scientific Reports, v. 7, p. 41164.

Wang, Y., Zheng, J., Zheng, Y., Liu, X., and Sun, G., 2015, Paleocene-Early Eocene uplift of the Altyn Tagh Mountain: Evidence from detrital zircon fission track analysis and seismic sections in the northwestern Qaidam basin: Journal of Geophysical Research: Solid Earth, v. 120, no. 12, p. 8534-8550.

Westerhold, T., Marwan, N., Drury Anna, J., Liebrand, D., Agnini, C., Anagnostou, E., Barnet James, S. K., Bohaty Steven, M., De Vleeschouwer, D., Florindo, F., Frederichs, T., Hodell David, A., Holbourn Ann, E., Kroon, D., Lauretano, V., Littler, K., Lourens Lucas, J., Lyle, M., Pälike, H., Röhl, U., Tian, J., Wilkens Roy, H., Wilson Paul, A., and Zachos James, C., 2020, An astronomically dated record of Earth's climate and its predictability over the last 66 million years: Science, v. 369, no. 6509, p. 1383-1387.

Wu, L., Xiao, A. C., Yang, S. F., Wang, L. Q., Mao, L. G., Wang, L., Dong, Y. P., and Xu, B., 2012, Two-stage evolution of the Altyn Tagh Fault during the Cenozoic: new insight from provenance analysis of a geological section in NW Qaidam Basin, NW China: Terra Nova, v. 24, no. 5, p. 387-395.

Ye, C., Yang, Y., Fang, X., and Zhang, W., 2016, Late Eocene clay boron-derived paleosalinity in the Qaidam Basin and its implications for regional tectonics and climate: Sedimentary Geology, v. 346, p. 49-59.

Ye, Y., Wu, L., Cowgill, E., Tian, Y., Lin, X., Xiao, A., and Chen, H., 2022, Long-lagged (~19 Myr) response of accelerated river incision to rock uplift on the northern margin of the Tibetan Plateau: Earth and Planetary Science Letters, v. 591, p. 117608.

Yin, A., Dang, Y. Q., Wang, L. C., Jiang, W. M., Zhou, S. P., Chen, X. H., Gehrels, G. E., and McRivette, M. W., 2008, Cenozoic tectonic evolution of Qaidam basin and its surrounding regions (Part 1): The southern Qilian Shan-Nan Shan thrust belt and northern Qaidam basin: Geological Society of America Bulletin, v. 120, no. 7-8, p. 813-846.

Yin, A., and Harrison, T. M., 2000, Geologic evolution of the Himalayan-Tibetan orogen: Annual Review of Earth and Planetary Sciences, v. 28, no. 1, p. 211-280.

Yin, A., Rumelhart, P., Butler, R., Cowgill, E., Harrison, T., Foster, D., Ingersoll, R., Qing, Z., Xian-Qiang, Z., and Xiao-Feng, W., 2002, Tectonic history of the Altyn Tagh fault system in northern Tibet inferred from Cenozoic sedimentation: Geological Society of America Bulletin, v. 114, no. 10, p. 1257-1295.

Yu, J., Zheng, D., Pang, J., Wang, Y., Fox, M., Vermeesch, P., Li, C., Xiao, L., Hao, Y., and Wang, Y., 2019, Miocene Range Growth Along the Altyn Tagh Fault: Insights From Apatite Fission Track and (U-Th)/He Thermochronometry in the Western Danghenan Shan, China: Journal of Geophysical Research: Solid Earth, v. 124, no. 8, p. 9433-9453.

Yue, Y. J., Graham, S. A., Ritts, B. D., and Wooden, J. L., 2005, Detrital zircon provenance evidence for large-scale extrusion along the Altyn Tagh fault: Tectonophysics, v. 406, no. 3, p. 165-178.

Yue, Y. J., Ritts, B. D., and Graham, S. A., 2001, Initiation and long-term slip history of the Altyn Tagh Fault: International Geology Review, v. 43, no. 12, p. 1087-1093.

Zhang, Z., Guo, Z., Li, J., and Tang, W., 2012, Mesozoic and Cenozoic uplift-denudation along the Altyn Tagh Fault, Northwestern China: Constrains from apatite fission track data: Quaternary Sciences, v. 32, no. 3, p. 499-509.

Zhuang, G., Johnstone, S. A., Hourigan, J., Ritts, B., Robinson, A., and Sobel, E. R., 2018, Understanding the geologic evolution of Northern Tibetan Plateau with multiple thermochronometers: Gondwana Research, v. 58, p. 195-210.

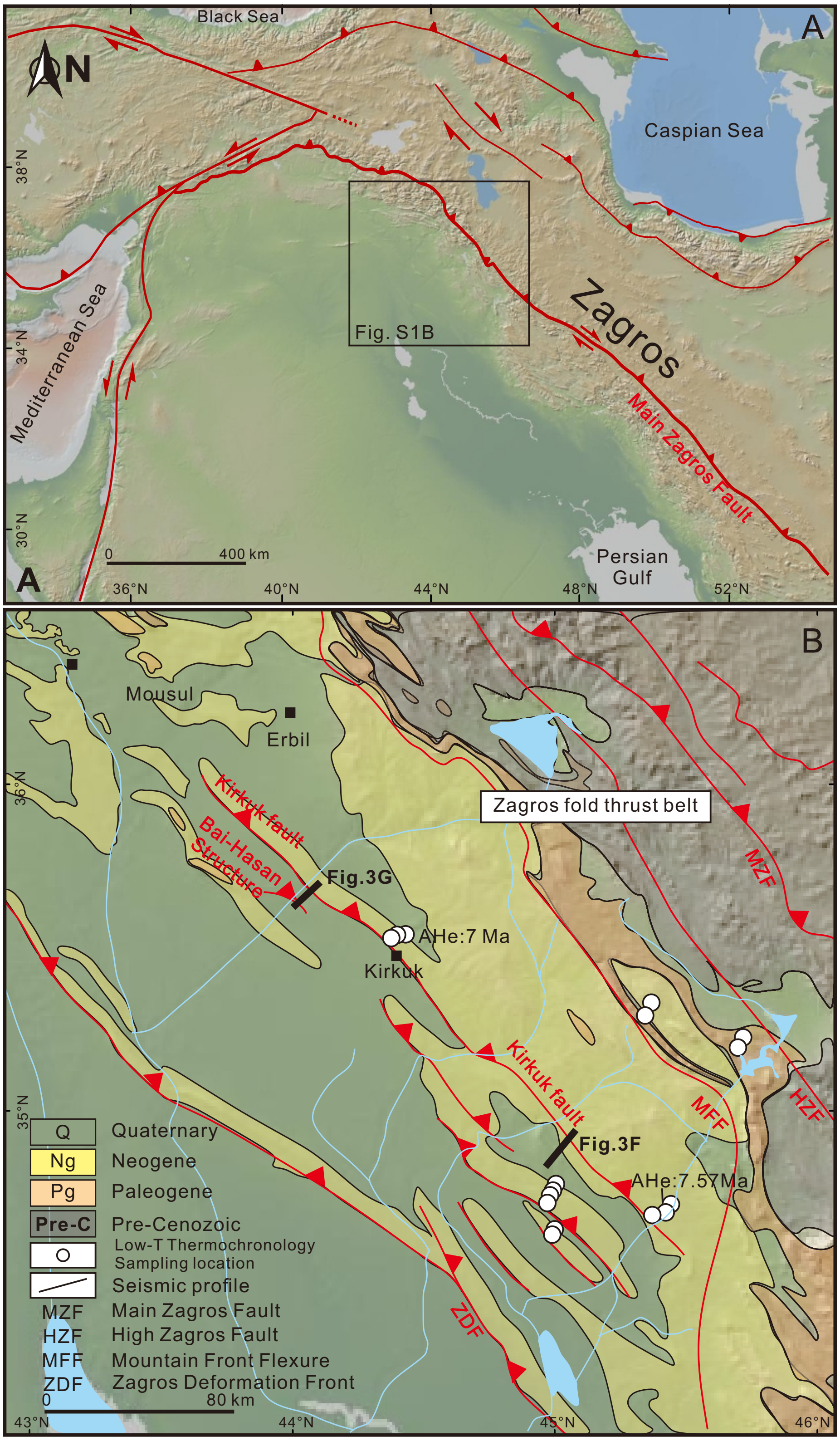

A
Black Sea
Caspian Sea
Mediterranean Sea
Zagros
Main Zagros Fault
Fig. S1B
Persian Gulf
0 400 km
36°N
40°N
44°N
48°N
52°N
30°N
34°N
38°N
B
Mousul
Erbil
Kirkuk
Kirkuk fault
Bai-Hasan Structure
Fig.3G
Fig.3F
AHe:7 Ma
AHe:7.57Ma
Zagros fold thrust belt
MZF
HZF
MFF
ZDF
Q Quaternary
Ng Neogene
Pg Paleogene
Pre-C Pre-Cenozoic
Low-T Thermochronology Sampling location
Seismic profile
MZF Main Zagros Fault
HZF High Zagros Fault
MFF Mountain Front Flexure
ZDF Zagros Deformation Front
0 80 km
43°N
44°N
45°N
46°N
35°N
36°N

Fig. S1

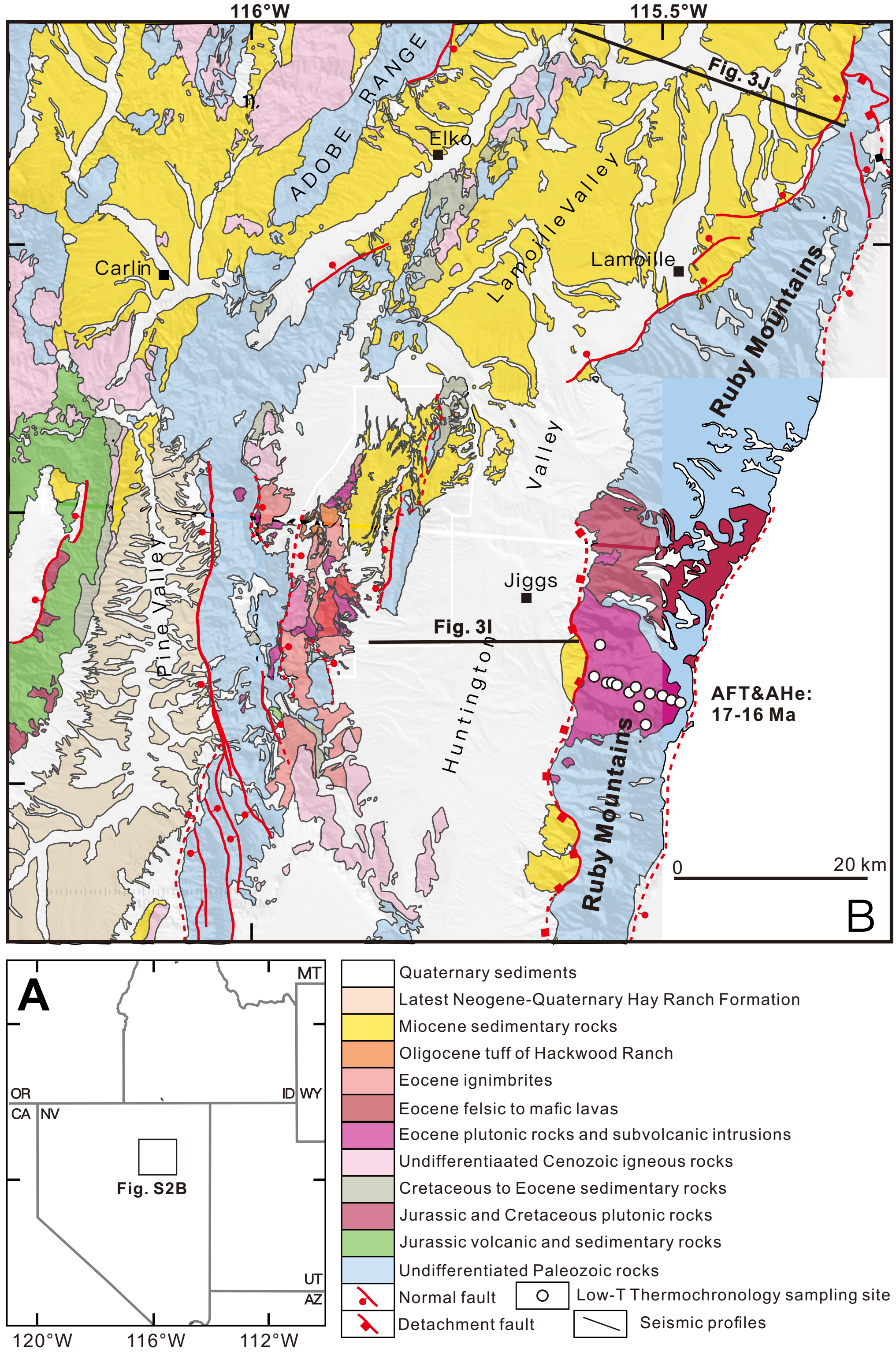
116°W
115.5°W
40.75°N
40.50°N
40.25°N
ADOBE RANGE
Elko
Carlin
Lamoille Valley
Lamoille
Ruby Mountains
Fig. 3J
Fig. 3I
Valley
Jiggs
Pine Valley
Huntington
AFT&AHe:
17-16 Ma
0
20 km
B
A
MT
OR
CA
NV
ID
WY
UT
AZ
44°N
40°N
Fig. S2B
120°W
116°W
112°W
Quaternary sediments
Latest Neogene-Quaternary Hay Ranch Formation
Miocene sedimentary rocks
Oligocene tuff of Hackwood Ranch
Eocene ignimbrites
Eocene felsic to mafic lavas
Eocene plutonic rocks and subvolcanic intrusions
Undifferentiaated Cenozoic igneous rocks
Cretaceous to Eocene sedimentary rocks
Jurassic and Cretaceous plutonic rocks
Jurassic volcanic and sedimentary rocks
Undifferentiated Paleozoic rocks
Normal fault
Low-T Thermochronology sampling site
Detachment fault
Seismic profiles

Fig. S2

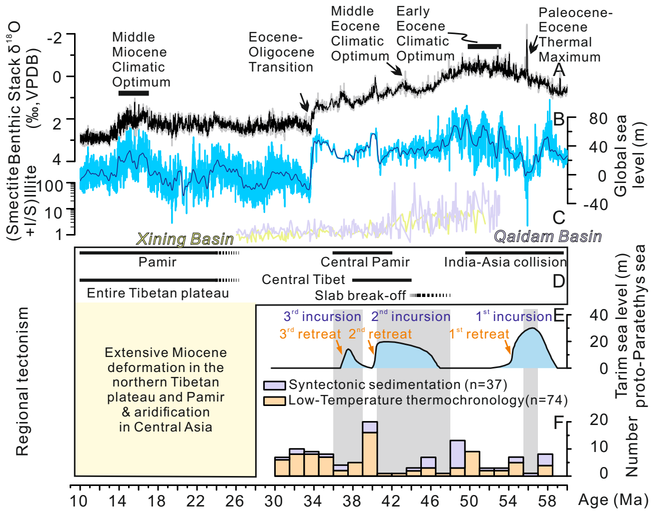

Middle Miocene Climatic Optimum
Eocene-Oligocene Transition
Middle Eocene Climatic Optimum
Early Eocene Climatic Optimum
Paleocene-Eocene Thermal Maximum
A
B
C
D
E
F
Benthic Stack δ18O (‰,VPDB)
Global sea level (m)
(Smectite +I/S)/Illite
Xining Basin
Qaidam Basin
Pamir
Central Pamir
India-Asia collision
Central Tibet
Entire Tibetan plateau
Slab break-off
Regional tectonism
Extensive Miocene deformation in the northern Tibetan plateau and Pamir & aridification in Central Asia
3rd incursion
2nd incursion
1st incursion
3rd retreat
2nd retreat
1st retreat
Tarim sea level (m) proto-Paratethys sea
Syntectonic sedimentation (n=37)
Low-Temperature thermochronology(n=74)
Number
Age (Ma)

Fig. S3

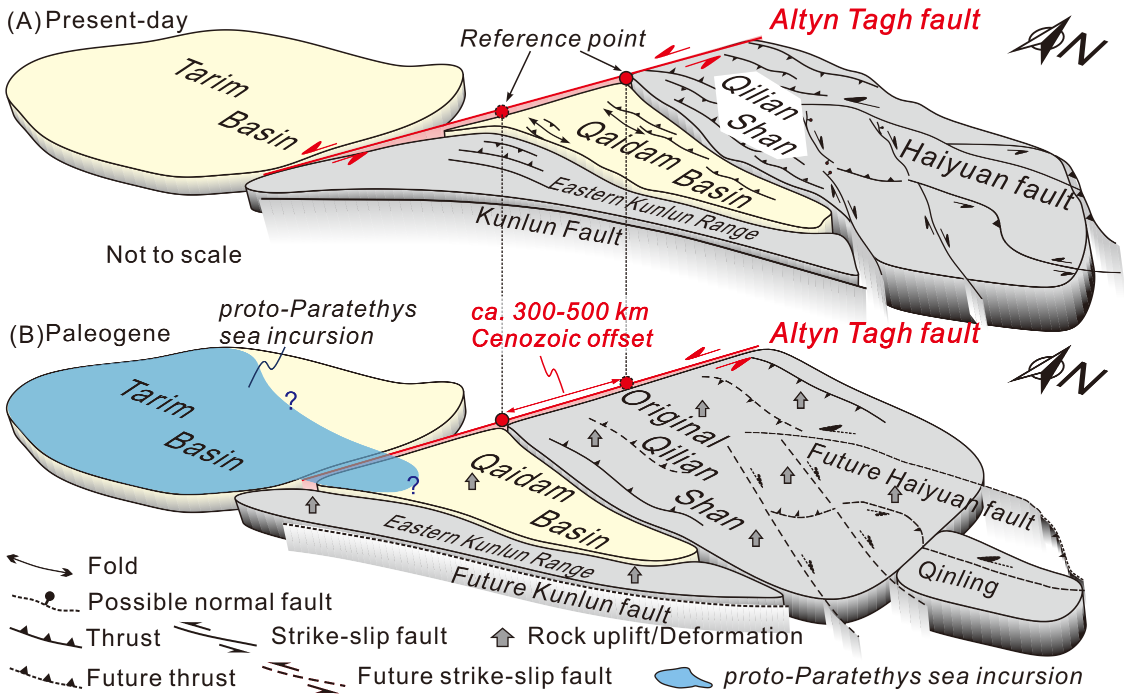

(A) Present-day
Tarim Basin
Reference point
Altyn Tagh fault
N
Qilian Shan
Qaidam Basin
Haiyuan fault
Eastern Kunlun Range
Kunlun Fault
Not to scale
(B) Paleogene
proto-Paratethys sea incursion
ca. 300-500 km Cenozoic offset
Altyn Tagh fault
N
Tarim Basin
Original Qilian Shan
Future Haiyuan fault
Qaidam Basin
Eastern Kunlun Range
Future Kunlun fault
Qinling
Fold
Possible normal fault
Thrust
Strike-slip fault
Rock uplift/Deformation
Future thrust
Future strike-slip fault
proto-Paratethys sea incursion

Fig. S4